

DIGITAL SIMULATION OF BRANCH-CONTROLLED DELTA-CONNECTED INDUCTION MOTOR

M.M. Ahmed

Department of Electrical Engineering, Faculty of Engineering,
Alexandria University, Alexandria, Egypt.

ABSTRACT

This paper presents a simplified model for digital simulation of a branch-controlled delta connected three-phase induction motor. The effect of changing the delay angle on motor torque/speed characteristic is investigated. Comparison is made between transient and steady state behaviours both when using branch-controlled delta-connection and when using line-controlled star-connection. Harmonic analysis for steady state torque, phase and line current are carried out.

LIST OF PRINCIPAL SYMBOLS

R_s, R_r	Stator and rotor phase resistance respectively (P.U.).
L_s, L_r, M	Apparent three phase stator, rotor and mutual inductance respectively (P.U.).
s, r	Suffixes indicating stator and rotor quantities.
$q, p, 0$	Suffixes indicating quadrature axis, direct axis and zero sequence quantities respectively.
V_{RS}	Voltage difference between terminals R and S (P.U.).
V_{RSoc}	Open circuit e.m.f. between R and S (P.U.).
$\dot{\theta}_r$	Rotor angular velocity (P.U.).
T_e, T_L, T_d	Electrical, load and drag torques respectively (P.U.).
T_x	Thyristor x.
T_xF	Logical trigger signal for T_x .
T_xC	Logical conduct signal for T_x .
V_xF	Logical forward bias signal for T_x .
I	Logical direction indicator for current i .
H	Logical magnitude indicator for i .
\bar{A}	A bar under a variable indicates the use of matrix notation.
\bar{H}	A bar above logical variable indicates the logic inverse "NOT (H)".

controlled three-phase star-connected induction motor is shown in Figure (1-a). If both ends of the motor stator windings are available there is possible advantage to be gained in considering the connection of Figure (1-b), which forms a branch-controlled delta-connected induction motor [5].

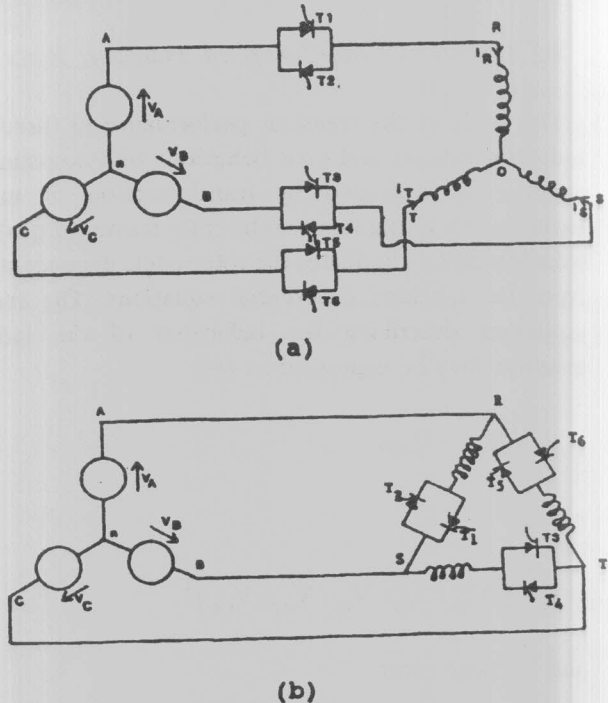


Figure 1. SCR voltage controller induction motor
(a) line-controlled star-connected motor
(b) branch-controlled delta-connected motor.

1. INTRODUCTION

SCR voltage controllers are increasingly used to control the speed of three-phase induction motors, especially in low power applications with variable load torques such as fans, blowers, and centrifugal pumps [1-5]. A typical line-

It has been shown [5] that the three-phase branch-controlled delta-connection results in a superior performance to that of line-controlled star-connection with both resistive and R-L loads, and there is a possibility to get the same superiority with motor loads.

Several authors have presented analyses models to predict the behaviour of line-controlled star-connected induction motor [6-8]. In previous work, the author presented a simplified technique for digital simulation of line-controlled star-connected induction motor [9]. This technique utilises the two phase time-invariant representation of an induction machine with respect to orthogonal stationary axes. In this paper a simplified model for digital simulation of branch-controlled delta-connected induction motor is presented based on the same previous technique. The model has been programmed using Pascal language. Comparison is made between the simulated results of branch-controlled delta-connected motor and line-controlled star-connected motor. The effects of changing the thyristor delay angle on the motor speed, efficiency and power factor in both cases are investigated. Harmonic analysis for steady state torque, phase current and line current are carried out.

2.1 Analysis of Delta-Connected induction Motor

The study of the transient performance of three-phase induction motors and their behaviour with non-sinusoidal supplies is facilitated by transformation of machine variables to a stationary reference frame (d-q-o). This transformation eliminates the rotor angle dependent terms from the machine differential equations. The resultant equations describing the behaviour of the induction machine may be expressed as [10]:

$$\underline{V} = \underline{R} \underline{i} + \underline{L} \underline{p} \underline{i} \tag{1}$$

where

$$\underline{V} = [V_{qs} \ V_{ds} \ V_{os} \ V_{qr} \ V_{dr}]^T$$

and for cage rotor

$$\underline{V} = [V_{qs} \ V_{ds} \ V_{os} \ 0 \ 0]^T$$

$$\underline{i} = [i_{qs} \ i_{ds} \ i_{os} \ i_{qr} \ i_{dr}]^T$$

$$\underline{R} = \begin{bmatrix} R_s & 0 & 0 & 0 & 0 \\ 0 & R_s & 0 & 0 & 0 \\ 0 & 0 & R_s & 0 & 0 \\ 0 & -\dot{\theta}_r M & 0 & R_r & -\dot{\theta}_r L_r \\ \dot{\theta}_r M & 0 & 0 & \dot{\theta}_r L_r & R_r \end{bmatrix},$$

$$\underline{L} = \begin{bmatrix} L_s & 0 & 0 & M & 0 \\ 0 & L_s & 0 & 0 & M \\ 0 & 0 & L_{os} & 0 & 0 \\ M & 0 & 0 & L_r & 0 \\ 0 & M & 0 & 0 & L_r \end{bmatrix}$$

$$L_{os} = L_s \ M$$

And the relationship between stator (d-q-o) terms and the real stator phase variables is given by:

$$\begin{bmatrix} V_{RS} \\ V_{ST} \\ V_{TR} \end{bmatrix} = \underline{C} \begin{bmatrix} V_{qs} \\ V_{ds} \\ V_{os} \end{bmatrix} \tag{2}, \quad \begin{bmatrix} i_{RS} \\ i_{ST} \\ i_{TR} \end{bmatrix} = \underline{C} \begin{bmatrix} i_{qs} \\ i_{ds} \\ i_{os} \end{bmatrix} \tag{3}$$

where

$$\underline{C} = \begin{bmatrix} 1 & 0 & 1 \\ -1/2 & -\sqrt{3}/2 & 1 \\ -1/2 & \sqrt{3}/2 & 1 \end{bmatrix}$$

Equation (1) can be rewritten as:

$$\underline{p} \underline{i} = \underline{L}^{-1} \underline{V} - \underline{L}^{-1} \underline{R} \underline{i}$$

where

$$\underline{L}^{-1} = \begin{bmatrix} -L_r/D & 0 & 0 & M/D & 0 \\ 0 & -L_r/D & 0 & 0 & M/D \\ 0 & 0 & 1/L_{os} & 0 & 0 \\ M/D & 0 & 0 & -L_s/D & 0 \\ 0 & M/D & 0 & 0 & -L_s/D \end{bmatrix}$$

$$D = M^2 - L_s L_r$$

The equation of motion is given by:

$$Jp\dot{\theta}_r + T_d + T_L = T_e$$

$$\text{i.e. } p\dot{\theta}_r = (T_e - T_L - T_d) / J \quad (5)$$

where $T_e = M (i_{qs} i_{dr} - i_{ds} i_{qr})$ p.u.

Equations (4) and (5) completely define the dynamic model for any transient analysis. These equations can be rearranged in state space format:

$$\dot{\underline{X}} = f(\underline{X}, \underline{V}), \quad (6)$$

where

$$\underline{X} = [i_{qs} \ i_{ds} \ i_{os} \ i_{qr} \ i_{dr} \ \dot{\theta}_r]^T, \text{ where}$$

$$x_1=i_{qs}, \ x_2=i_{ds}, \ x_3=i_{os}, \ x_4=i_{qr}, \ x_5=i_{dr} \ \text{and} \ x_6=\dot{\theta}_r$$

Equations (6) are non-linear equations and numerical integration techniques are required to predict the system performance. For each integration step, stator phase voltages (V_{RS} , V_{ST} , and V_{TR}) can be determined according to the state of the thyristors.

2.2 Analysis of branch-controller

The conduction state of each thyristor, at any instant, can be determined as follows:

- i- If the thyristor is forward biased and its gate is excited it will conduct.
- ii- If the thyristor is already in conducting state and its current is in the forward direction and greater than its holding value, it continues to conduct.
- iii- Otherwise it will turn-off.

In Boolean terms:

$$T1C = T1F \vee 1F + T1C \cdot IR \cdot HR \quad (7.a)$$

$$T2C = T2F \cdot \bar{V}1F + T2C \cdot IR \cdot HR \quad (7.b)$$

$$T3C = T4F \vee 3F + T3C \cdot IS \cdot HS \quad (7.c)$$

$$T4C = T4F \cdot \bar{V}3F + T4C \cdot \bar{I}S \cdot \bar{H}S \quad (7.d)$$

$$T5C = T5F \vee 5F + T5C \cdot IT \cdot HT \quad (7.e)$$

$$T6C = T6F \cdot \bar{V}5F + T6C \cdot \bar{I}T \cdot \bar{H}T \quad (7.f)$$

From Figure (1-b), it can be seen that:

- i- V1F is true if V_{AB} is greater than V_{RSoc}
- ii- V3F is true if V_{BC} is greater than V_{SToc}
- iii- V5F is true if V_{CA} is greater than V_{TRoc}

According to the thyristors conducting states, the stator phase voltages (V_{RS} , V_{ST} and V_{TR}) can be determined as follows:

- i- If T1 or T2 is conducting then V_{RS} is equal to V_{AB} , otherwise it is equal to the open circuit e.m.f. V_{RSoc} .
- ii- If T3 or T4 is conducting then V_{ST} is equal to V_{BC} , otherwise it is equal to the open circuit e.m.f. V_{SToc} .
- iii- If T5 or T6 is conducting then V_{TR} is equal to V_{CA} , otherwise it is equal to the open circuit e.m.f. V_{TRoc} .

2.3 Calculation of open circuit e.m.f.'s

To calculate the e.m.f. that appears across any phase when it is opened, as a function of system state variables, one of the following three cases may be considered:

case 1- All three phases are open circuited simultaneously

In this case $i_R = i_S = i_T = 0$, which means that $i_{qs} = i_{ds} = i_{os} = 0$, i.e. $x_1 = x_2 = x_3 = 0$, and $px_1 = px_2 = px_3 = 0$.

Substitution into equations (6) and (2) gives

$$V_{RSoc} = Mx_5x_6 - (R_r M/L_r)x_4 \quad (8.a)$$

$$V_{SToc} = (R_r M / 2L_r)(x_4 + \sqrt{3}x_5) - 1/2 M x_6 (x_5 - \sqrt{3}x_4) \quad (8.b)$$

$$V_{TRoc} = (R_r M / 2L_r)(x_4 + \sqrt{3}x_5) - 1/2 M x_6 (x_5 - \sqrt{3}x_4) \quad (8.c)$$

case 2- Two phase are open circuited simultaneously

i) With phase ST and TR opened,

$$i_{ST} = i_{TR} = 0 \text{ and } V_{RS} = V_{AB}$$

Substitution into equation (3) gives

$$i_{qs} = 2 i_{os} \text{ and } i_{ds} = 0, \text{ i.e.}$$

$$x_1 = 2 x_3 \text{ and } x_2 = 0, \text{ and consequently}$$

$$px_1 = 2 px_3 \text{ and } px_2 = 0$$

Substitution into equation (6) and (2) gives

$$V_{SToc} = V_{AB} - (\sqrt{3}/2) (V_{ds} + \sqrt{3} V_{qs}) \quad (9.a)$$

$$V_{TRoc} = V_{AB} + (\sqrt{3}/2) (V_{ds} - \sqrt{3} V_{qs}) \quad (9.b)$$

where

$$V_{ds} = -M (x_4 + (M/L_r) x_1) x_6 - (R_r M / L_r) x_5$$

$$V_{qs} = (L_{os} R_s L_r x_1 - L_{os} R_r M x_4 + L_{os} L_r M x_5 x_6 + 2R_s D x_3 - 2D v_{AB}) / (L_{os} L_r - 2D).$$

ii) With phases RS and TR opened, V_{RSoc} and V_{TRoc} are found to be,

$$V_{RSoc} = V_{BC} + ((\sqrt{3}/2) (V_{ds} + \sqrt{3} V_{qs})) \quad (10.a)$$

$$V_{TRoc} = V_{BC} + \sqrt{3} V_{ds} \quad (10.b)$$

where

$$V_{qs} = \{L_{os} L_r R_s x_1 + (L_{os} - 3D/2L_r)(M^2 x_2 x_6 R_r M x_4 + L_r M x_5 x_6) + R_s D x_3 - (\sqrt{3}D/2L_r)(R_r M x_5 + L_r M x_4 x_6 + M^2 x_1 x_6) + D v_{BC}\} / (L_{os} L_r - 2D).$$

$$V_{ds} = (M/L_r) \{ \sqrt{3} (M x_2 x_6 - R_r x_4 + L_r x_5 x_6) - R_r x_5 - L_r x_4 x_6 - M x_1 x_6 \} + \sqrt{3} V_{qs}.$$

iii) With phases RS and ST opened, V_{RSoc} and V_{SToc} are found to be,

$$V_{RSoc} = V_{CA} - (\sqrt{3}/2) (V_{ds} - \sqrt{3} V_{qs}) \quad (11)$$

$$V_{SToc} = V_{CA} - \sqrt{3} V_{ds} \quad (12)$$

where

$$V_{qs} = \{L_{os} L_r R_s x_1 + (L_{os} - 3D/2L_r)(M^2 x_2 x_6 - R_r M x_4 + L_r M x_5 x_6) - R_s D x_3 + \sqrt{3} D / 2L_r (R_r M x_5 + L_r M x_4 x_6 + M^2 x_1 x_6) + D v_{CA}\} / (L_{os} L_r - 2D).$$

$$V_{ds} = (M/L_r) \sqrt{3} (M x_2 x_6 + R_r x_4 + L_r x_5 x_6) - R_r x_5 - L_r x_4 x_6 - M x_1 x_6 \sqrt{3} V_{qs}.$$

case 3- One phase only is open circuited

i) With phase RS circuited

$$i_R = 0, V_{ST} = V_{BC} \text{ and } V_{TR} = V_{CA}.$$

Substitution into equation (3) gives

$$i_{qs} = -i_{os}, \text{ i.e. } x_1 = -x_3$$

and consequently $px_1 = -px_3$.

Substituting into equations (6) and (2) gives

$$V_{RSoc} = \{(3L_{os})(R_s L_r x_1 - R_r M x_4 + M^2 x_2 x_6 + L_r M x_5 x_6) - R_s D x_3 + M(L_r - M) V_{AB}\} / (2L_{os} L_r - D). \quad (12)$$

ii) With phase ST open circuited V_{SToc} is found to be,

$$V_{SToc} = \{(3L_{os}/2)(R_r M x_4 - R_s L_r x_1 - M^2 x_2 x_6 - L_r M x_5 x_6) + \sqrt{3} R_r M x_5 - \sqrt{3} R_s L_r x_2 + \sqrt{3} M^2 x_1 x_6 - 3R_s D x_3 - M(L_r - M) V_{BC}\} / (2L_{os} L_r - D).$$

iii) With phases TR open circuited V_{TRoc} is found to be,

$$V_{TRoc} = \{(3L_{os}/2)(R_r M x_4 - R_s L_r x_1 - M^2 x_2 x_6 - L_r M x_5 x_6) + \sqrt{3} R_r M x_5 + \sqrt{3} R_s L_r x_2 - \sqrt{3} M^2 x_1 x_6 - \sqrt{3} L_r M x_4 x_6 - 3R_s D x_3 - M(L_r - M) V_{CA}\} / (2L_{os} L_r - D). \quad (14)$$

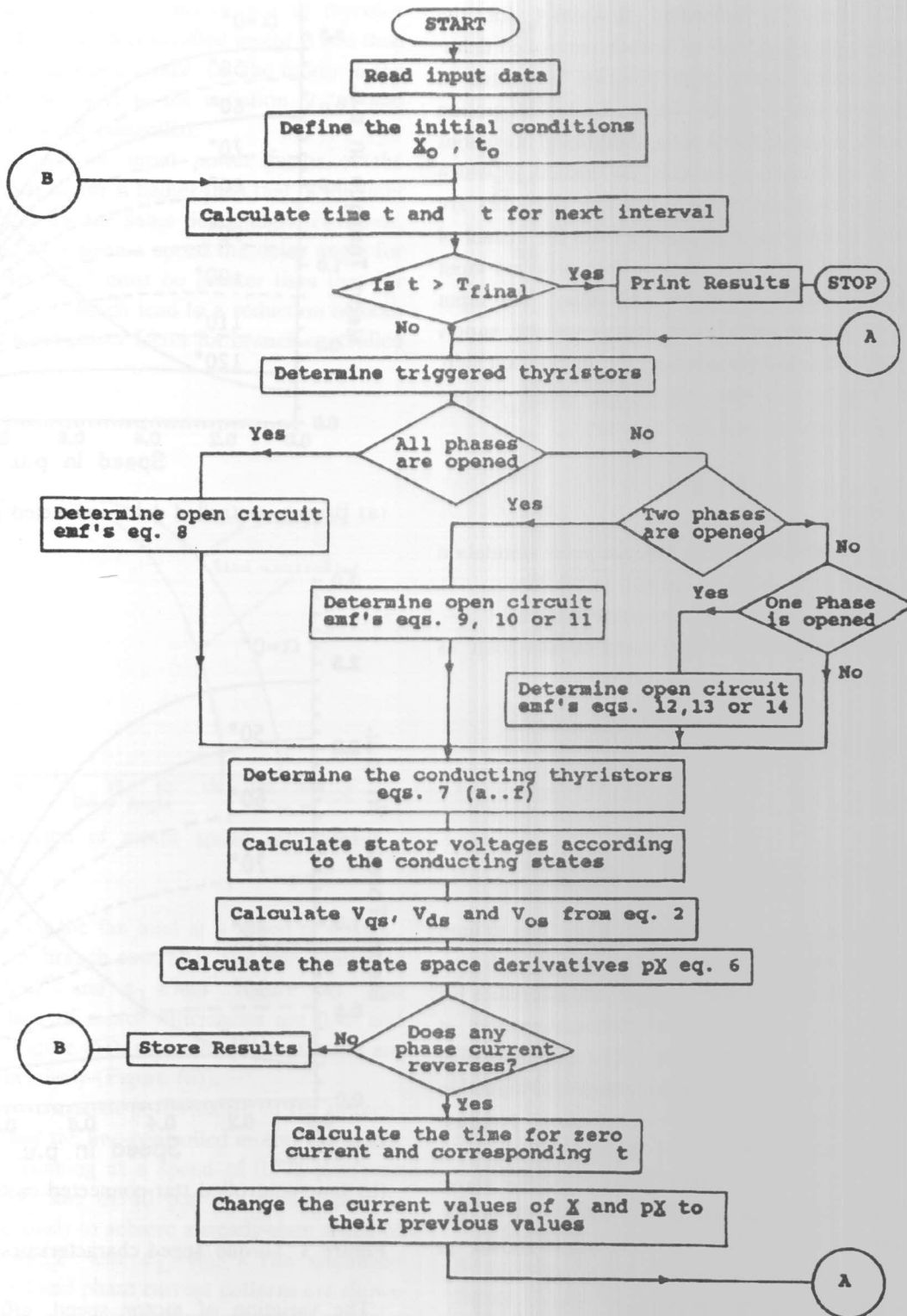


Figure 2. Program flow-chart.

3. COMPUTER SIMULATION PROGRAM

Figure (2) shows a simplified flow-chart for the computer simulation program of branch-controlled delta connected induction motor. The program is written in pascal and uses fourth order Runge-Kutta integration algorithm with nominal fixed step. Additional iterations were used to determine accurately the instant at which thyristors were fired and extinguished. The thyristors are triggered with a delay angle measured from the instant of voltage-zero of the respective phases. Both program input data and output results are in per unit values. The input data are the machine parameters, supply voltage, supply frequency thyristors delay angle, and the integration step. The output results comprises the motor speed, torque, voltages, phase currents, and line currents.

4. RESULTS AND DISCUSSION

The motor parameters used for the computer simulation program are the same as those quoted in [6]: viz 1/3 hp, 220 v, 50Hz, 4 pole, wound-rotor machine. The motor parameters in per unit using rated voltage as base voltage and 375 watts as base power are.

$$R_s = 0.0566 \text{ p.u. } R_r = 0.1252 \text{ p.u.}$$

$$L_s = 1.0318 \text{ p.u. } L_r = 1.0318 \text{ p.u.}$$

$$M = 0.969 \text{ p.u. } J_r = 3.0 \text{ p.u.}$$

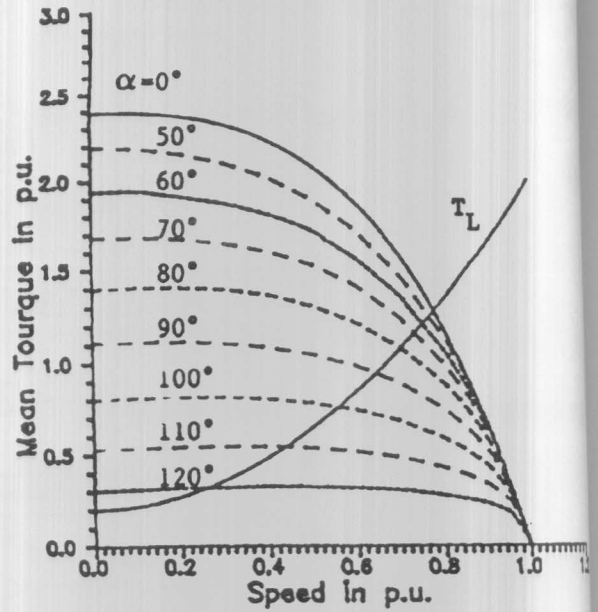
It is assumed that 1 p.u. peak supply voltage (line to line) is applied to the motor.

Figure (3-a) Shows the torque/speed characteristics for the motor with branch-controlled delta-connection at different values of delay angle "α". The corresponding characteristics for line-controlled star-connected induction motor were obtained using the simulation program presented by the author in [9].

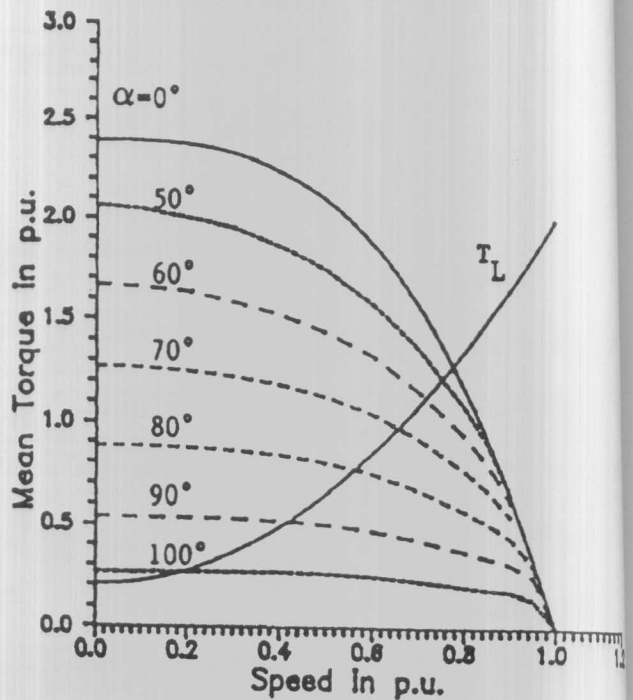
Figure (3-b) shows these characteristics for the above motor with the same applied phase voltage as in the branch-controlled case. The characteristics shown in Figure (3-b) are identical to those given in [6].

For a fan load with a torque equation:

$$T_L = 0.2 + 1.8 (\text{speed})^2 \text{ p.u}$$



(a) Branch controlled delta-connected motor.



(b) Line-controlled star-connected motor.

Figure 3. Torque/speed characteristics.

The variation of motor speed, efficiency, and input power factor with the thyristor delay angle "α" for both branch-controlled and line-controlled motor is shown in

Figure (4), (5) and (6) respectively. From these curves it can be seen that:

- i) The speed rate of change, with respect to thyristor delay angle, of the branch-controlled motor is less than that of the line-controlled motor, i.e. the motor in the first case is less sensitive to the variation of " α " and therefore easier to be controlled.
- ii) The efficiency and the input power factor of the branch controlled motor is higher than that of the line-controlled motor for the same delay angle. However, to run the load at a certain speed the delay angle for branch-controller " α_B " must be greater than that for line-controller " α_L ", which lead to a reduction of both efficiency and input power factor for branch-controlled motors.

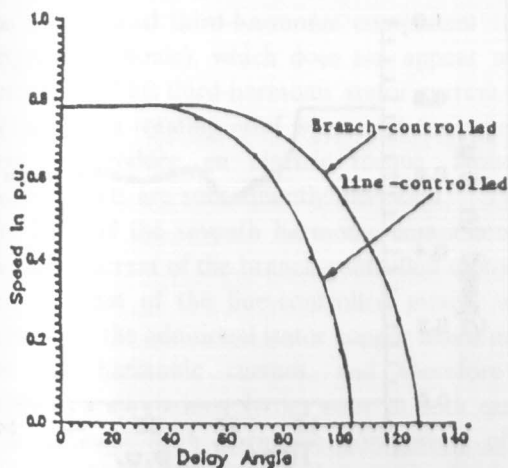


Figure 4. Variation of motor speed with delay angle " α ".

For example to run the fan load at a speed of 0.6 p.u., the delay angles for branch-controller and line-controller must be $\alpha_B = 95.2^\circ$ and $\alpha_L = 76.3^\circ$ Figure (4). The corresponding values of motor efficiencies are 0.47 and 0.48 respectively (Figure (5)), while the power factors are 0.72 and 0.74 respectively (Figure (6)).

To compare the transient performance of the branch-controlled motor and the line-controlled motor, the motor is assumed to be running at a speed of 0.775 p.u. (zero delay angle). At a time of 10 p.u. the delay angle is changed instantaneously to achieve a steady-state speed of 0.6 p.u., i.e. $\alpha_B = 95.2^\circ$ and $\alpha_L = 76.3^\circ$. The simulated motor torque, speed and phase current patterns are shown in Figure (7) for the branch-controlled delta-connected motor and in Figure (8) for the line-controlled star-connected motor.

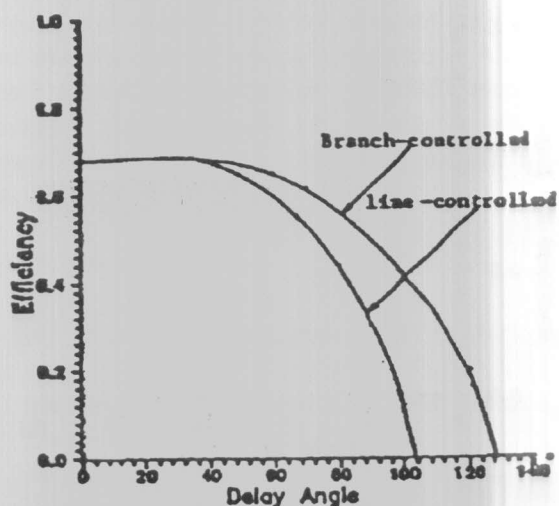


Figure 5. Variation of motor efficiency with delay angle " α ".

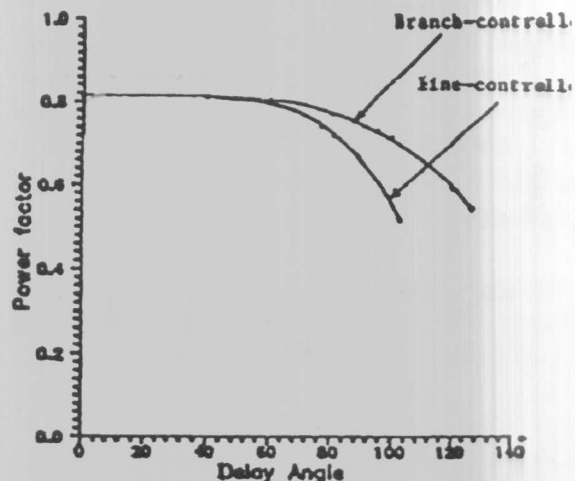


Figure 6. Variation of input power factor with delay angle " α ".

Comparison between transient responses for both cases (Figure (7) and (8)) shows that:

- i) The pulsating torque in the branch-controlled motor is less than that in the line-controlled motor.
- ii) The branch-controlled motor is more damped than the line-controlled motor.
- iii) The phase-current in the branch-controlled motor is higher than that in the line-controlled motor.

By applying fourier analysis to the simulated waveforms of Figure (7 and 8), the amplitude of harmonic components for the torque, phase current and line current after reaching steady-state conditions were calculated.

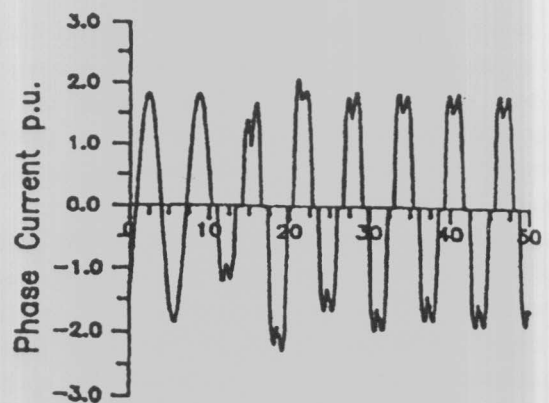
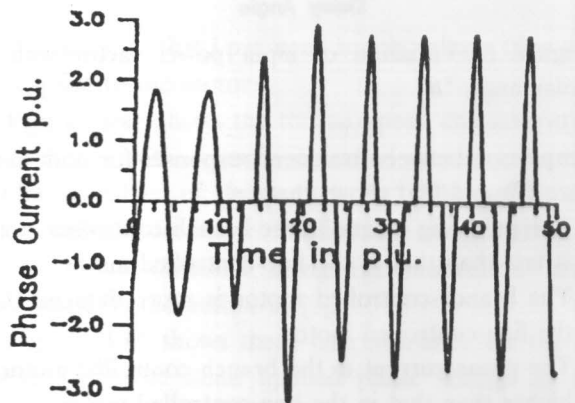
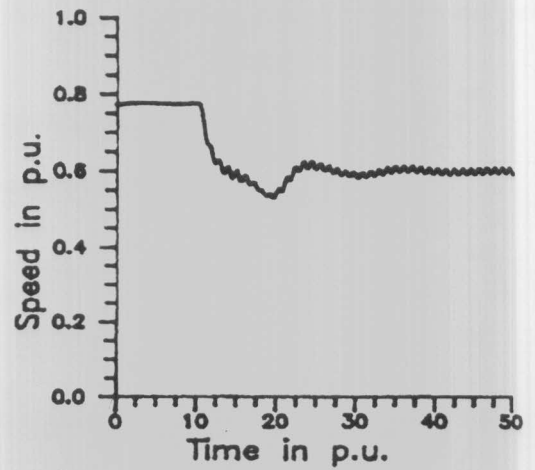
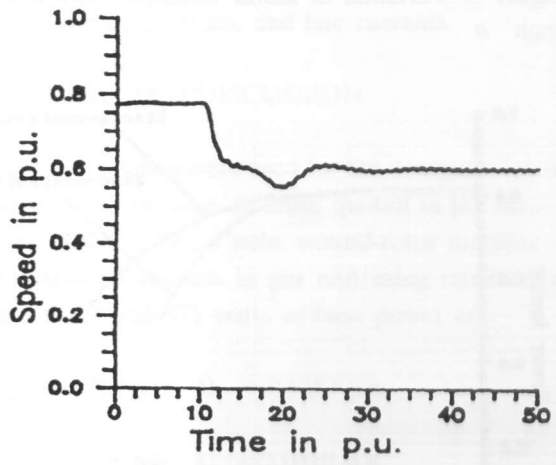
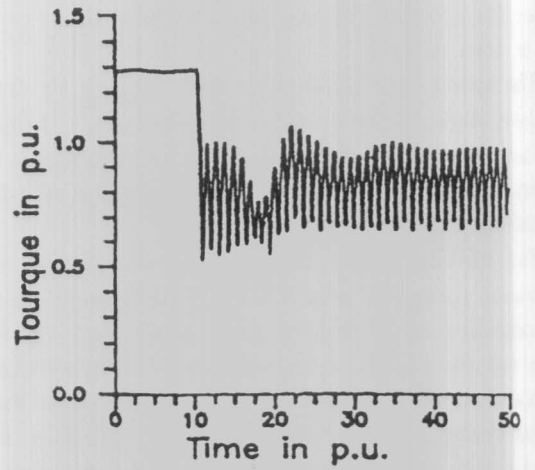
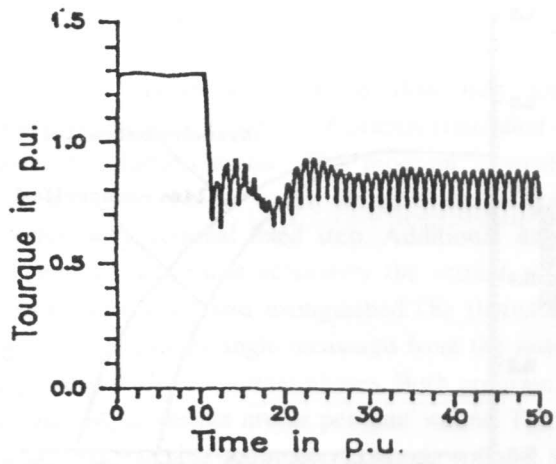


Figure 7. Simulated results for branch-controlled motor

Figure 8. Simulated results for line-controlled motor

Table 1. Amplitude of harmonic components in p.u.

Harmonics No.	Torque		Phase Current		Line Current	
	Branch	Line	Branch	Line	Branch	Line
0	0.848	0.848	0.0	0.0	0.0	0.0
1	0.0	0.0	1.844	1.836	3.182	1.836
3	0.0	0.0	0.96	0.0	0.0	0.0
5	0.0	0.0	0.088	0.401	0.161	0.401
6	0.061	0.144	0.0	0.0	0.0	0.0
7	0.0	0.0	0.141	0.177	0.240	0.177
9	0.0	0.0	0.049	0.0	0.0	0.0
12	0.010	0.004	0.0	0.0	0.0	0.0

The results are summarized in Table(1) and they show that:

- i) The phase current in the branch-controlled motor has a substantial third-harmonic component (zero-sequence harmonic), which does not appear in the line current. This third-harmonic stator current does not produce a rotating mmf wave, and consequently does not produce an electric torque. However, heating effects are subsequently increased.
- ii) The fifth and the seventh harmonic components in the phase current of the branch-controlled motor are less than that of the line-controlled motor, which compensate the additional stator copper losses due to the third harmonic current, and therefore the efficiency is approximately the same in both cases.
- iii) The dominant sixth harmonic component of the torque in the branch-controlled motor is about 58% less than that in the line-controlled motor. This result was expected since the sixth harmonic torque is developed from the interaction between the magnetizing current and both fifth and seventh harmonic phase currents.

5. CONCLUSIONS

An efficient method of predicting the performance of branch-controlled delta-connected induction motor has been presented.

A comparison between a branch-controlled delta-connected induction motor and a line-controlled star-connected induction motor has been made. This comparison shows that the branch-controlled motor has a superior performance to that of the line-controlled motor. It has been shown that the branch-controlled motor is easier to be controlled, since it has a lower rate of change

of speed with respect to thyristors delay angle. It is also more damped and has less pulsating torque. Although the phase current of the branch controlled motor has a substantial third harmonic component, its efficiency is slightly decreased since its fifth and seventh harmonic components are greatly reduced.

6 REFERENCES

- [1] P.C. Sen, *Power Electronic*, TATA McGraw Hill, 1987.
- [2] S.B. Dewan and A. Straughen, *Power semiconductor drives* Wiley, New York, 1984.
- [3] W. Shepherd, *Thyristors control of ac circuits*, Bradford University press, 1975.
- [4] M.H. Rashid, *Power Electronic*, Prentice-Hall, 1988.
- [5] W. Shepherd, *Power Electronics & motor control*, Cambridge University Press, 1988.
- [6] T.A. Lipo, "The analysis of induction motor with voltage control by symmetrically triggered thyristors", *IEEE Trans. on PAS.*, Vol. PAS-90, pp. 515-525, March 1971.
- [7] G. Nath and G. Berg, "Transient analysis of three phase SCR controlled induction motor", *IEEE Trans. on LA.* Vol. LA-17, No. 2, pp. 133-142, March/April 1981.
- [8] S. Murthy and G. Berg, "A new approach to modelling and transient analysis of SCR controlled induction motor", *IEEE Trans. on PAS*, Vol. PAS-101, No. 9, pp. 3141-3150, Sep. 1982.
- [9] M.M. Ahmed, "Digital simulation of SCR voltage controlled induction motor", *Proceeding International conference signal and system*, Al-Ain (U.A.E.), Jan. 1990, AMSE Press, Vol. 2, pp. 107-118.
- [10] P. Krause and C. Thomas, "Simulation of symmetrical induction machinery", *IEEE Trans. on PAS*, Vol. PAS-84, pp. 1038-1053, Nov. 1965.